Research on Engineering Structures & Materials
www.jresm.org
MIM Research Group

Research Article

Mechanistic assessment of ductile and brittle failure predictions for Balau SWS bolted connections in timber diaphragm retrofit applications

Erwan Sukarman [*,1,a], Abdul Razak Abdul Karim [1,b], Norazzlina M.Sa'don [1,c], Abdul Azim Abdullah [1,d], Siti Hanim Sahari [2,e], Teng Xin Yao [2,f], Nur Liza Rahim [3,g], Pierre Quenneville [4,h]

[1]*Faculty of Engineering, Universiti Malaysia Sarawak (UNIMAS), Malaysia*
[2]*Research, Development and Innovation Division, Forest Department Sarawak (FDS), Malaysia*
[3]*Faculty of Civil Engineering Technology, Universiti Malaysia Perlis (UniMAP), Malaysia*
[4]*Faculty of Engineering, The University of Auckland (UoA), New Zealand*

Article Info

Article History:

Received 28 Jul 2026

Accepted 12 Oct 2026

Keywords:

Bolted timber connection;
Balau wood;
Optimized design;
Strength prediction;
Unreinforced masonry retrofit

Abstract

Unreinforced masonry (URM) buildings with timber diaphragms are vulnerable to seismic loading where inadequate wall–diaphragm connections compromise structural integrity. Current MS544-5 provisions do not explicitly incorporate key material parameters and failure mechanisms relevant to dense tropical hardwoods, while mechanistically based models remain insufficiently assessed across ductile and brittle failure regimes. This study addresses this gap by experimentally investigating steel–wood–steel (SWS) bolted connections in Balau (Shorea spp.) and evaluating the European Yield Model (EYM), Row Shear Model (RSM), and MS544-5 against experimental 5th-percentile resistances. Eighteen connection configurations were tested under monotonic tension with varying end distances and bolt spacings. The average and 5th-percentile embedding strengths were 52.32 and 24.11 MPa, respectively, while the 5th-percentile oven-dry density was 679 kg/m^3. For ductile-failure configurations, the EYM yielded a mean prediction ratio of 0.62 compared with 0.39 for MS544-5. For brittle row-shear configurations, the calibrated RSM (CF = 4.9) yielded 0.72 compared with 0.63 for MS544-5. The findings demonstrate that mechanistically based formulations provide closer agreement with experimental characteristic resistances and support more representative assessment of Balau bolted connections for timber diaphragm retrofit applications, subject to further independent and cyclic validation.

© 2026 MIM Research Group. All rights reserved.

1. Introduction

Unreinforced masonry (URM) buildings are widely recognized as highly vulnerable to seismic loading due to inadequate structural connectivity, particularly the absence of effective wall–diaphragm connections [1-10]. This deficiency frequently leads to out-of-plane wall failure and, in severe cases, partial or total structural collapse [1- 4]. The vulnerability is further exacerbated in buildings incorporating timber floor and roof diaphragms, where insufficient anchorage between structural components significantly reduces structural integrity and seismic resistance [5, 6, 9, 10].

In Malaysian practice, bolted timber connections are commonly employed in timber diaphragm systems; however, their design is governed by MS544-5 [11], which is based on simplified assumptions and lacks essential material parameters for local hardwoods. Consequently, the

*Corresponding author: 22010316@siswa.unimas.my
[a]orcid.org/0009-0000-6827-8189; [b]orcid.org/0000-0001-5631-834X; [c]orcid.org/0000-0001-8567-823X; [d]orcid.org/0000-0002-7081-7062; [e]orcid.org/0009-0007-3273-2571; [f]orcid.org/0009-0004-3913-7749; [g]orcid.org/0000-0001-6609-8512; [h]orcid.org/0000-0002-7470-9990
DOI: http://dx.doi.org/10.17515/resm2026-2051ma0728rs

resulting design predictions are often overly conservative and may not accurately represent the true structural capacity of the connections. Previous investigations on Malaysian hardwoods, including Meraka, Nyatoh, and Bitis, have demonstrated that bolted connection behavior is governed by both ductile embedding-controlled mechanisms and brittle row shear failure, depending on geometric parameters such as end distance and bolt spacing [12-16]. Similar observations have also been reported in international studies, where brittle failure susceptibility was shown to increase in connections with insufficient geometric spacing, multiple fasteners and reduced end distances [17-23].

Current timber design provisions, particularly MS544-5 [11], implicitly favor ductile behavior and do not explicitly account for brittle row shear mechanisms. Although advanced analytical approaches such as the European Yield Model (EYM) and Row Shear Model (RSM) provide improved predictive capability through mechanistic representation of connection behavior [17-23], their implementation remains dependent on species-specific material parameters, including embedding strength and density. Furthermore, the performance of existing mechanistically based analytical models for dense tropical hardwoods remains insufficiently assessed across both ductile and brittle governing failure conditions. In particular, limited information is available on whether the European Yield Model (EYM) and Row Shear Model (RSM), when implemented using experimentally derived material properties, can provide a more representative assessment of Balau bolted connection resistance than the simplified provisions of MS544-5. This limitation is particularly relevant to retrofit applications involving existing or heritage structures, where timber species and their corresponding material properties may be difficult to establish due to ageing, degradation, and limited construction documentation [5, 10, 24]. Consequently, a systematic experimental assessment is required to establish appropriate material parameters and evaluate failure-mechanism-specific prediction approaches for dense tropical hardwood connections.

Therefore, this study experimentally investigates the behavior of steel–wood–steel (SWS) bolted connections using Balau wood (Shorea spp.), a Strength Group 1 hardwood classified under MS544-2 [25]. The objectives are to:

- determine the key Balau material properties required for mechanistically based resistance prediction;
- evaluate the predictive performance of the EYM, RSM, and MS544-5 against experimentally determined 5th-percentile connection resistances for ductile and brittle failure configurations; and
- determine an appropriate Balau-specific calibration factor for the RSM under brittle row-shear failure.

The novelty of this study lies in the integrated experimental and mechanistic assessment of Balau SWS bolted connections across both ductile embedding/bolt-yielding and brittle row-shear failure regimes using experimentally derived material properties. Unlike an assessment based solely on code-prescribed parameters, the present study directly relates the experimentally observed failure mechanisms to the corresponding EYM and RSM formulations and quantitatively evaluates their agreement with experimental 5th-percentile resistances relative to MS544-5. The resulting Balau-specific material parameters and calibrated row-shear formulation provide a mechanistic basis for more representative assessment of bolted hardwood connections relevant to timber diaphragm retrofit applications. However, the calibrated RSM factor is limited to the experimental domain investigated and requires independent validation before broader design generalization.

2. Methodology

2.1 Identification of Wood Species

Timber specimens used in this study were obtained from Balau wood, commonly referred to as Selangan Batu, which belongs to the Dipterocarpaceae family and is scientifically classified as Shorea spp. According to MS544-2 [25], Balau is categorized under Strength Group 1 (SG1), representing high-density hardwoods with superior mechanical properties suitable for structural applications [26]. To ensure the reliability of the experimental results, genus verification of the

timber specimens was conducted using end-grain microscopic examination. Specimens were prepared following established procedures, and cross-sectional surfaces were examined at a magnification of 20× to capture the anatomical features of the wood. The observed characteristics (refer to Figure 1) include small to medium vessel sizes (<100 μm), predominantly solitary vessel arrangement with occasional radial multiples, and the presence of tyloses. Both apotracheal and paratracheal parenchyma were identified, with the former appearing as irregular concentric bands and the latter as incomplete vasicentric patterns. Rays were visible with a typical frequency of approximately 6–9 rays per mm. These anatomical observations are consistent with reported anatomical characteristics of Dipterocarp hardwood species [27]. These anatomical features are consistent with documented characteristics of Balau wood [28] and were further verified through comparison with reference samples obtained from the Wood Library of the Forest Department Sarawak (FDS) as shown in Figure 2. The agreement between observed and reference features confirms that the timber specimens used in this study belong to the Shorea spp. genus.

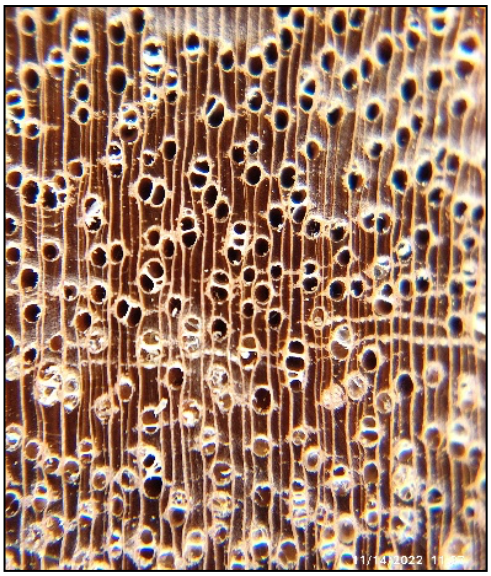

Fig. 1. End-grain section of Balau wood examined at 20× magnification



Fig. 2. Reference Balau wood specimen verified by the Wood Library, Research, Development and Innovation Division, Forest Department Sarawak (FDS)

2.2 Testing Program

This study involves the experimental determination of key material and connection parameters required for evaluating the strength of bolted timber connections using the European Yield Model (EYM) and the Row Shear Model (RSM). The primary parameters include moisture content, density, embedding strength, and connection strength under tensile loading parallel to the grain. All tests were conducted in accordance with relevant international standards to ensure consistency and reliability. Moisture content and density were determined following AS/NZS 1080.1 [29] and AS/NZS 1080.3 [30], respectively, while embedding strength was evaluated in accordance with ISO 10984-2 [31]. Bolted connection tests were performed using a steel–wood–steel (SWS) double-shear configuration under monotonic tensile loading. The experimental program was structured to capture both ductile and brittle failure behavior by varying key geometric parameters, namely end distance (e_t) and bolt spacing (s_b). These parameters are known to significantly influence the governing failure mode of bolted connections. Detailed procedures for specimen preparation, connection configuration, and test setup are presented in the following sections.

2.3 Bolted Connection Test

2.3.1 Specimen Preparation and Configuration Details

Bolted connection specimens were prepared using Balau timber in a steel–wood–steel (SWS) double-shear configuration. The timber members had a cross-section of 50 mm × 100 mm and were

fabricated as single-row bolted connections. Grade 4.6 steel bolts with a nominal diameter, d, of 13 mm were installed in 14-mm-diameter pre-drilled holes. The timber member was sandwiched between two 16-mm-thick mild-steel side plates. The steel plates served as a rigid loading fixture and were proportioned such that deformation or failure of the steel plates would not govern the measured connection resistance; hence, the plate length and width were not considered experimental variables in this study.

Identical connection configurations were provided at both ends of each specimen, with a longitudinal separation of l_4 = 400 mm between the two connection regions. This distance satisfied the minimum requirement of $l_4 \geq 30d = 390$ mm for the 13-mm-diameter bolt and was adopted to promote independent behavior of the connections at the two specimen ends. A single-row bolt arrangement was used, satisfying the transverse edge-distance requirement of $a_1 \geq 3d = 39$ mm. The principal geometric variables investigated were the end distance, e_t, bolt spacing, s_b, and number of bolts, n_f. The end distance varied from 50 to 150 mm, while the longitudinal bolt spacing was 50 or 100 mm, depending on the connection configuration. In this study, n_f denotes the number of bolts per connection end, with n_f = 1, 2, and 3 corresponding to one-, two-, and three-bolt arrangements, respectively. The same connection configuration was duplicated at the opposite end of each specimen. The complete configurations of the eighteen connection groups are summarized in Table 1, while the specimen geometry and dimensional parameters are illustrated in Figure 3. The test program was designed to investigate the influence of these geometric parameters on connection resistance and failure behavior, with particular emphasis on the transition between ductile embedding/bolt-yielding behavior and brittle row-shear failure. End distance and bolt spacing were selected as principal variables because they significantly influence the governing failure mechanism of bolted timber connections [18, 20, 21, 22]. These two failure regimes also correspond directly to the analytical formulations evaluated in this study: the European Yield Model (EYM) represents ductile behavior governed by timber embedding and fastener yielding, whereas the Row Shear Model (RSM) represents brittle resistance governed by shear failure parallel to the grain. Other potential brittle failure modes in bolted timber connections, including splitting, net tension, and group tear-out, were recognized but were not treated as separate predictive failure modes in the present analytical assessment. Failure classification was based on the experimentally observed governing mechanism at the connection resistance. Where local splitting or other cracking developed only after the governing resistance had been reached, it was regarded as secondary damage rather than the controlling failure mechanism. Accordingly, the analytical comparison was restricted to connection configurations experimentally governed by ductile embedding/bolt yielding or brittle row shear. The resulting EYM and RSM assessments should therefore be interpreted within these experimentally observed failure regimes and should not be generalized to connection configurations governed by splitting, net tension, or group tear-out.

To minimize material sampling bias and account for the inherent variability of hardwood, the specimens within each connection group were fabricated from different timber planks. This precaution reduced the likelihood of obtaining replicate specimens from the same timber source and improved the representativeness of the experimental dataset. Each of the eighteen connection groups comprised ten replicate specimens, providing the experimental basis for evaluating the effects of connection geometry and for subsequent comparison with the analytical strength predictions.

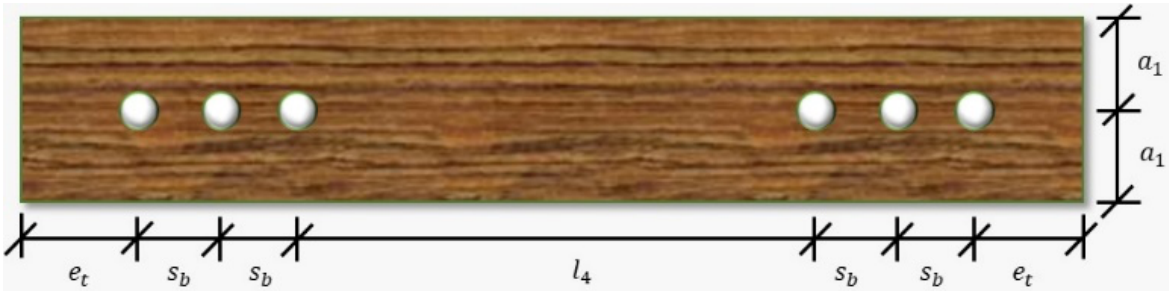

Fig. 3. Geometry and dimensional variables of the SWS bolted connection specimen

Table 1. Bolted connection specimen configuration details

Group	End distance, e_t (mm)	Spacing of bolts, s_b (mm)	Number of bolts per connection end, n_f
1	150	-	1
2	125	-	1
3	100	-	1
4	75	-	1
5	50	-	1
6	150	100	2
7	125	100	2
8	100	100	2
9	75	100	2
10	50	100	2
11	150	50	2
12	125	50	2
13	100	50	2
14	75	50	2
15	50	50	2
16	100	50	3
17	75	50	3
18	50	50	3

Note: n_f denotes the number of bolts within one connection end considered in the resistance calculation. The corresponding bolt arrangement was provided symmetrically at the opposite end of the test specimen.

2.3.2 Experimental Setup and Procedures

The bolted connection tests were conducted using a steel-wood-steel (SWS) double-shear configuration, where timber members were sandwiched between two steel plates to ensure uniform load transfer. The steel plates, each 16 mm thick, were designed to remain elastic throughout testing, thereby ensuring that failure occurred within the timber components, consistent with common timber connection testing practice [18, 20, 23]. The connections were assembled using grade 4.6 steel bolts, with nuts tightened to a snug-fit condition to avoid introducing pre-stress effects. The number of bolts varied according to the connection configuration. All specimens were tested under monotonic tensile loading parallel to the grain using a universal testing machine with a capacity of 300 kN. The loading was applied at a constant displacement rate of 1 mm/min until failure, in accordance with ISO 6891 [32]. Load-displacement data were continuously recorded for each specimen, and the ultimate load was taken as the maximum resistance achieved prior to failure. Failure modes were visually inspected and documented, and representative failure patterns were recorded for analysis.

2.4 Determination of Wood Material Properties

The material properties required for the analytical prediction of bolted connection strength, namely embedding strength, density, and moisture content, were determined experimentally. These parameters form the fundamental inputs for the European Yield Model (EYM) and Row Shear Model (RSM), respectively. The testing program was conducted in accordance with relevant international standards to ensure consistency and reliability. The experimentally derived embedding strength and density parameters are presented and discussed in Section 3.1, where their implications for strength prediction are evaluated.

2.4.1 Embedding Strength Test

The embedding strength of Balau wood was determined in accordance with ISO 10984-2 [31], as this parameter governs the resistance prediction of bolted connections in the EYM formulation. Test specimens were extracted from the timber members used in the bolted connection tests to maintain material consistency. Each specimen was prepared with dimensions satisfying the minimum geometric requirements of the standard, including a specimen height of 100 mm, exceeding the minimum requirement of 7d for the 13 mm bolt diameter used, as illustrated in

Figure 4. A steel dowel of matching diameter was loaded in compression at a displacement rate of 1 mm/min until failure. Figure 5 shows the typical embedding strength test setup. The embedding strength was determined from the maximum applied load divided by the bearing area, corresponding to the projected contact area between the dowel and the timber specimen. The resulting values were subsequently used as input parameters for evaluating the predictive performance of the EYM.

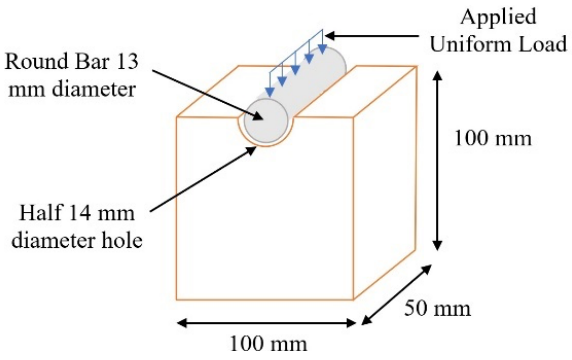

Fig. 4. Geometry of the embedding strength test specimen



Fig. 5. Experimental setup for the embedding strength test

2.4.2 Moisture Content and Density Tests

Oven-dry density and moisture content were determined in accordance with AS/NZS 1080.3 [30] and AS/NZS 1080.1 [29], respectively. Test samples were extracted from the bolted connection specimens to ensure representative material characterization. Each specimen measured 20 mm × 50 mm × 10 mm and was initially weighed prior to oven drying at 103 ± 2°C until constant mass was achieved. Based on the testing program, stable mass conditions were generally attained after three days of drying. Moisture content was calculated from the difference between initial and oven-dry mass, while oven-dry density was determined from the ratio of dry mass to specimen volume. The measured density values were subsequently used to estimate the shear strength parallel to the grain through the adopted correlation for RSM predictions. The measured moisture content verifies that all specimens satisfy the dry timber condition specified in MS544-2 [25].

2.5 Statistical Analysis and Model Performance Metrics

2.5.1 Determination of Characteristic Values

The experimental results were statistically characterized using the arithmetic mean, standard deviation (s), and coefficient of variation (CoV). The CoV was calculated by using Eq. (1):

$$CoV = (s/\bar{X}) \times 100\% \tag{1}$$

where s is the sample standard deviation and $\bar{X}$ is the sample mean.

For the purpose of comparison with characteristic-level analytical resistance predictions, the lower 5th-percentile value was estimated parametrically assuming an approximately normal distribution of the measured property within the relevant dataset. The characteristic value was calculated by using Eq. (2):

$$X_{5th} = \bar{X} - 1.645s \tag{2}$$

or equivalently Eq. (3),

$$X_{5th} = \bar{X}[1 - 1.645(CoV/100)] \tag{3}$$

where X_{5th} is the estimated lower 5th-percentile value and 1.645 is the one-sided standard-normal variate corresponding to the lower 5% probability level. This procedure was applied consistently to the experimentally determined embedding strength and connection resistance datasets. The resulting 5th-percentile values were subsequently adopted as characteristic experimental inputs for comparison with the EYM, RSM, and MS544-5 predictions.

2.5.2 Model Performance Metrics

The agreement between the analytical strength predictions and the experimentally derived characteristic resistances was evaluated by using Eq. (4), the prediction ratio (PR). For each connection group, the prediction ratio was calculated as:

$$PR_i = \frac{R_{pred,i}}{R_{exp,5th,i}} \tag{4}$$

where $R_{pred,i}$ is the analytical predicted resistance and $R_{exp,5th,i}$ is the estimated experimental 5th-percentile resistance for connection group i. The overall agreement across the investigated connection groups was represented by using Eq. (5) the mean prediction ratio:

$$\overline{PR} = \frac{1}{n}\sum_{i=1}^{n} PR_i \tag{5}$$

where n is the number of connection groups considered. A prediction ratio of PR = 1.0 represents exact agreement between the analytical prediction and experimental characteristic resistance. Values of PR < 1.0 indicate conservative predictions, whereas PR > 1.0 indicates unconservative overprediction. The mean prediction ratio was used to quantify the overall level of agreement and conservatism across the investigated connection groups.

To provide complementary measures of prediction error, the mean absolute percentage error (MAPE), Eq (6), and root mean square error (RMSE), Eq. (7), were also calculated as follows:

$$MAPE = \frac{100}{n}\sum_{i=1}^{n} \frac{R_{pred,i} - R_{exp,5th,i}}{R_{exp,5th,i}} \tag{6}$$

$$RMSE = \sqrt{\frac{1}{n}\sum_{i=1}^{n}\left(R_{pred,i} - R_{exp,5th,i}\right)^2} \tag{7}$$

Lower MAPE and RMSE values indicate closer agreement between the analytical predictions and experimental characteristic resistances. These error metrics were considered together with the prediction ratio because PR additionally indicates whether a prediction is conservative or unconservative, which is particularly relevant for structural design applications.

3. Results and Discussion

This section presents and discusses the experimentally determined material properties of Balau wood, together with the observed failure behavior and predictive performance of the analytical models considered. Particular emphasis is placed on the mechanistic interpretation of ductile and brittle failure modes, and on evaluating the predictive performance of the European Yield Model (EYM), Row Shear Model (RSM), and MS544-5 provisions in predicting bolted connection resistance. Both experimental average and 5th-percentile values of the measured material properties and connection capacities were determined to support comparison with design-level strength predictions. In particular, the 5th-percentile embedding strength was adopted in the EYM analysis, while the 5th-percentile oven-dry density was used to derive the shear strength parameter required for the RSM predictions. This approach ensures consistency with characteristic design resistance concepts and enables direct evaluation of the predictive performance of the analytical models against experimentally observed connection strengths.

In addition to assessing prediction accuracy, the discussion examines the influence of geometric parameters, particularly end distance (e_t) and bolt spacing (s_b), on governing failure mechanisms and the transition between ductile embedding-controlled behavior and brittle row shear failure, with the results further interpreted in the context of connection mechanics and design applicability for timber diaphragm retrofitting.

3.1 Wood Properties

The experimentally determined material properties of Balau wood are summarized in Tables 2 and 3, including embedding strength, oven-dry density, and moisture content. These parameters are fundamental to the analytical prediction of bolted connection strength, as embedding strength governs the resistance estimation in the European Yield Model (EYM), while oven-dry density provides the basis for deriving the shear strength parameter used in the Row Shear Model (RSM). The measured average embedding strength, $f_{h,avg}$, of 52.32 MPa and characteristic 5th-percentile value, $f_{h,5th\%}$, of 24.11 MPa indicate the high bearing resistance of Balau wood, consistent with its classification as a Strength Group 1 hardwood. The coefficient of variation (CoV) of 32.78% reflects the natural heterogeneity commonly associated with timber and is comparable to variability reported for hardwood embedding strength in previous studies [12, 13, 14, 15, 16]. The characteristic embedding strength adopted in this study provides the critical input parameter for evaluating the predictive performance of the EYM.

The density results show an average oven-dry density, ρ_{avg}, of 799 kg/m^3 and a 5th-percentile value, $\rho_{5th\%}$, of 679 kg/m^3, confirming the high-density nature of Balau wood. These density values were used to estimate the shear strength parallel to the grain through the adopted density-strength correlation, forming the principal input for RSM predictions. The relatively low CoV of 9.15% indicates limited dispersion in density compared with embedding strength, suggesting a comparatively stable basis for brittle failure modelling. The use of experimentally derived characteristic properties rather than code-prescribed surrogate parameters enables a more direct assessment of model reliability for local hardwood connections. The measured average moisture content of 16% confirms that all specimens were tested under dry timber conditions in accordance with MS544-2, ensuring consistency with the assumptions underlying the adopted design models. The influence of moisture variation on connection strength was therefore not considered within the scope of the present study. Overall, the experimentally derived material parameters provide the basis for evaluating both ductile and brittle strength predictions and support the development of reliable and optimized design parameters for Balau bolted connections.

Table 2. Experimental embedding strength results for Balau wood

Hardwood	No. of specimens	$f_{h,avg}$ (MPa)	CoV (%)	$f_{h,5th\%}$ (MPa)
Balau	175	52.32	32.78	24.11

Table 3. Experimental moisture content and density results for Balau wood

Hardwood	No. of specimens	ρ_{avg} (kg/m3)	CoV (%)	$\rho_{5th\%}$ (kg/m3)	MC_{avg} (%)
Balau	198	799.4	9.15	679	16

3.2 Failure Mode Observations

3.2.1 Ductile Failure Mode

For connection groups with end distance and bolt spacing equal to or greater than 75 mm (Groups 1–4 and 6–9), the dominant response was characterized by ductile behavior governed primarily by embedding deformation of the timber and yielding of the steel bolt. Typical failure observations (Figure 6) show enlargement of the bolt hole accompanied by visible bolt bending, indicating mobilization of both wood bearing resistance and fastener plastic deformation. This response is consistent with the expected ductile failure mechanisms described by the European Yield Model [17, 18, 19], where connection resistance is governed by the interaction between timber

embedding strength and bolt bending capacity. Although local row shear or splitting was occasionally observed at ultimate stages, these occurred as secondary phenomena after the governing connection capacity had been reached and therefore did not control the failure resistance.

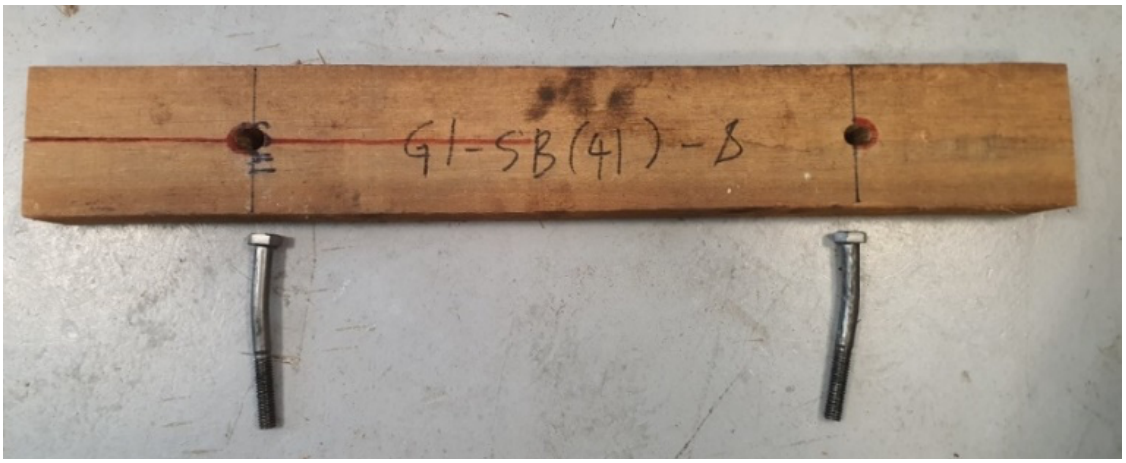

Fig. 6. Observed ductile failure of the bolted connection for Group 1 (e_t = 150 mm)

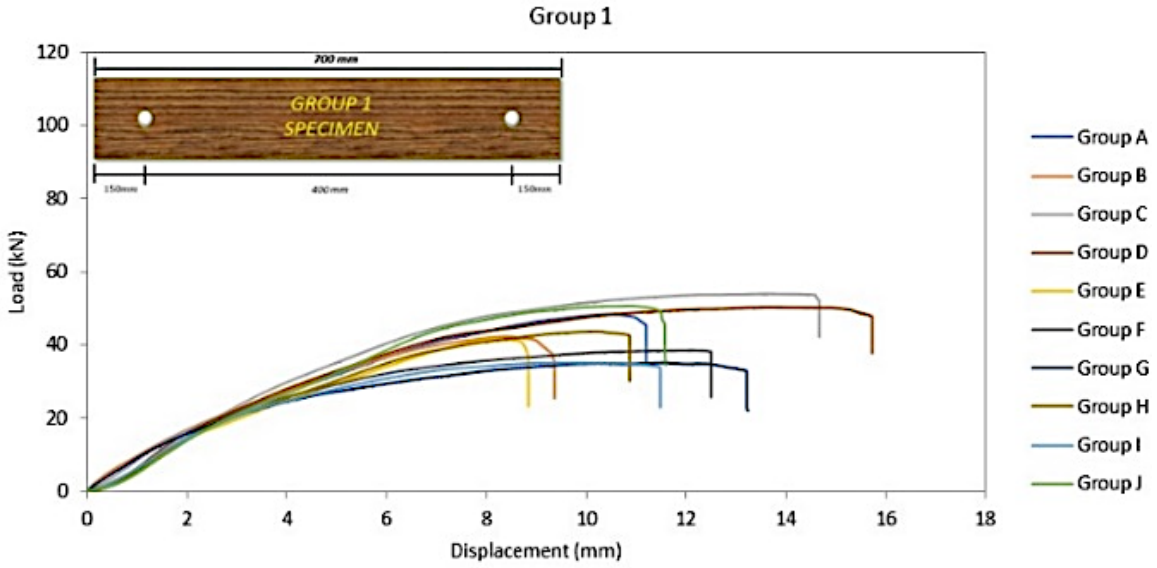

Fig. 7. Load-displacement curves for Group 1 (e_t = 150 mm)

The corresponding load-displacement responses (Figure 7) further confirm ductile behavior through progressive load development, significant deformation capacity, and the formation of post-yield plateaus indicative of strain hardening. Such behavior demonstrates stable deformation capacity under monotonic loading, which is a desirable connection characteristic for timber diaphragm retrofit applications [5, 10]. However, the observed monotonic response should not be interpreted as direct evidence of cyclic energy-dissipation capacity or seismic performance. These observations indicate that sufficiently large end distances and bolt spacing promote redistribution of stresses and delay the onset of brittle shear failure, thereby favoring embedding-controlled ductile response.

3.2.2 Brittle Failure Mode

In contrast, connections with end distance and/or bolt spacing equal to 50 mm (Group 5 and Groups 10–18) predominantly failed in brittle row shear parallel to the grain, as shown in Figure 8. In these configurations, geometric constraints restricted the development of embedding deformation and shifted the governing resistance mechanism towards shear failure of the timber. Unlike ductile failures, brittle row shear was characterized by abrupt crack propagation parallel to the grain with little observable bolt yielding or hole deformation, indicating that the embedding strength and fastener bending resistance were not fully mobilized prior to failure. This confirms

that the governing mechanism in these configurations was controlled by timber shear resistance rather than ductile interaction mechanisms.

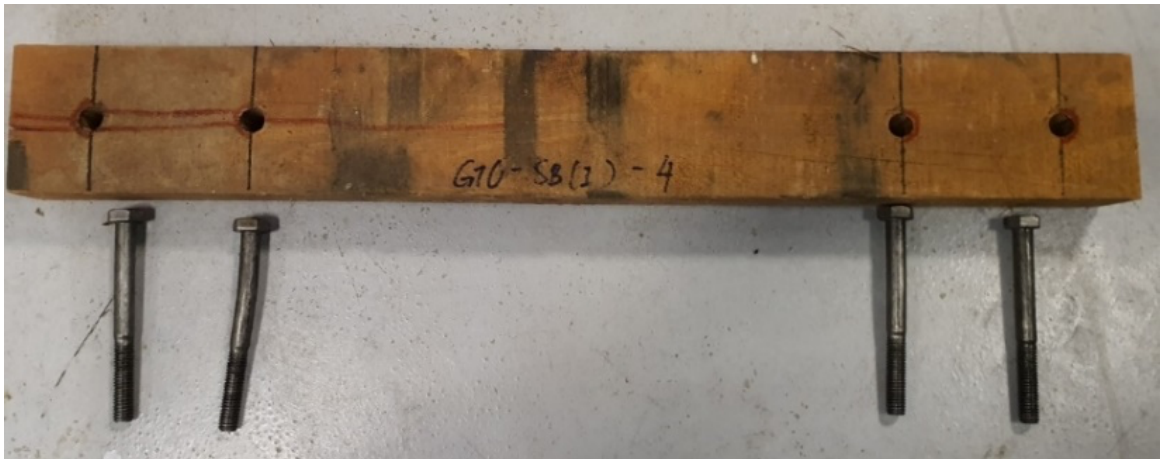

Fig. 8. Observed brittle row-shear failure of the bolted connection for Group 10 (e_t = 50 mm, s_b = 100 mm)

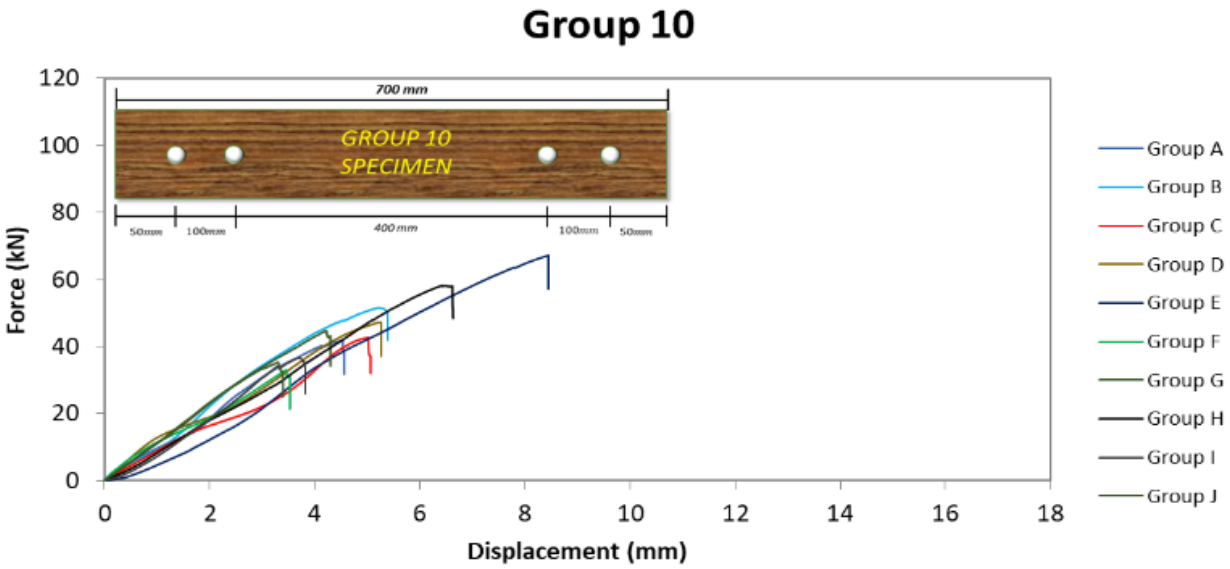

Fig. 9. Load-displacement curves for Group 10 (e_t = 50 mm and s_b = 100 mm)

The brittle response is further reflected in the load-displacement curves (Figure 9), where sudden load drops occurred at relatively small displacements without the formation of a plastic plateau. This behavior is characteristic of unstable failure and limited deformation capacity, consistent with brittle row shear behavior reported in previous timber connection studies [20, 21, 22]. The results confirm that geometric parameters, particularly end distance and bolt spacing, govern the transition between ductile and brittle response. Connections with reduced geometric spacing exhibit increased susceptibility to row shear failure, highlighting the importance of geometry as a controlling design parameter in bolted timber connections.

Accordingly, the subsequent predictive assessment was restricted to the experimentally identified governing mechanisms of ductile embedding/bolt yielding and brittle row shear; other potential brittle failure mechanisms, including splitting, net tension, and group tear-out, were outside the analytical scope of the present study. The experimentally observed transition between these governing failure mechanisms therefore provides the basis for the subsequent failure-mode-specific assessment of the EYM and RSM.

3.2.3 Predictive Performance under Ductile Failure: EYM versus MS544-5

The predictive performance of the European Yield Model (EYM) and MS544-5 for connection groups governed by ductile failure (Groups 1–4 and 6–9) is summarized in Table 4 and illustrated in Figure 10. Comparison between predicted strengths and the estimated 5th-percentile resistances shows that EYM consistently provides closer agreement with experimental results than the current timber code provisions.

For Balau bolted connections, the EYM prediction ratios ranged from 0.47 to 0.81, with a mean prediction ratio of 62%, whereas MS544-5 yielded substantially lower ratios ranging from 0.30 to 0.51, corresponding to a mean prediction ratio of 39%. The consistently higher prediction ratios obtained using the EYM indicate closer agreement with the experimental 5th-percentile resistances than those obtained using MS544-5. Notably, the prediction hierarchy observed, with EYM consistently outperforming MS544-5 across all ductile groups, confirms the robustness of embedding-strength-based design formulations for local hardwood connections.

The EYM yielded a mean prediction ratio of 0.62, with a MAPE of 38.33% and RMSE of 18.64 kN, whereas MS544-5 yielded a lower mean prediction ratio of 0.39, together with a higher MAPE of 61.12% and RMSE of 27.42 kN. Thus, within the investigated ductile-failure configurations, the EYM exhibited smaller deviations from the experimental characteristic resistances, while both approaches remained conservative on average.

As shown in Figure 10, the predictions from MS544-5 fall considerably below the one-to-one reference line, indicating systematic conservatism. In contrast, EYM predictions exhibit closer alignment with the experimental data, although remaining on the conservative side, which is desirable from a structural design perspective.

The improved performance of EYM is attributed to its mechanistic representation of ductile connection behavior [17, 18, 19], where resistance is governed by the interaction between timber embedding deformation and bolt bending. The conservatism of MS544-5 may be attributed to the absence of explicit embedding strength parameters, which limits its ability to capture the enhanced bearing resistance of dense tropical hardwood bolted connections. This mechanistically explains the systematically lower prediction ratios obtained for MS544-5 relative to EYM across all ductile connection groups.

The results are consistent with previous findings reported for other Malaysian hardwoods, including Meraka [12], Nyatoh [14], and Bitis [16], indicating that the predictive advantage of EYM is not species-specific but reflects a broader mechanistic validity in modelling ductile behavior of bolted timber connections. These findings support the use of embedding-strength-based prediction models for improved and less conservative design of timber diaphragm connections in URM retrofit applications.

Table 4. Comparison of EYM and MS544-5 predictions with experimental results for ductile-failure configurations of Balau bolted connections

Group	Experimental			Predictions		PR		EYM vs MS544-5		
	R_{avg} (kN)	CoV (%)	$R_{5th\%}$ (kN)	EYM (kN)	MS544-5 (kN)	EYM $R_{5th\%}$	MS544-5 $R_{5th\%}$	$\overline{PR}$	MAPE (%)	RMSE (kN)
1	43.99	15	33.01	15.67	9.88	0.47	0.30			
2	37.87	24	23.16	15.67	9.88	0.68	0.43			
3	38.93	21	25.40	15.67	9.88	0.62	0.39			
4	38.27	30	19.28	15.67	9.88	0.81	0.51	0.62 vs 0.39	38.33 vs 61.12	18.64 vs 27.42
6	77.53	22	49.42	31.34	19.76	0.63	0.40			
7	86.83	21	56.76	31.34	19.76	0.55	0.35			
8	91.93	18	64.98	31.34	19.76	0.48	0.30			
9	77.09	25	45.81	31.34	19.76	0.68	0.43			

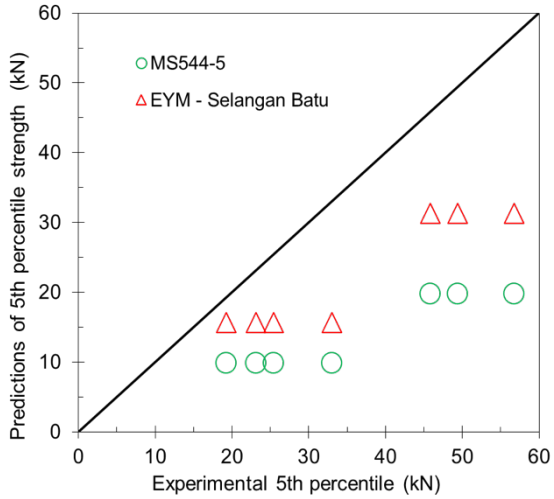

Fig. 10. Comparison of EYM and MS544-5 predictions with experimental 5th-percentile resistances for ductile-failure configurations

3.2.4 Determination and Assessment of Calibration Factor for Balau Wood

The calibration factor for Balau wood was determined using the connection configurations governed experimentally by brittle row-shear failure, namely Group 5 and Groups 10–18. For each configuration, the calibration factor required for the RSM-predicted resistance to equal the corresponding experimental 5th-percentile resistance was determined. The resulting factors ranged from approximately 2.38 to 4.86, with Group 18 producing the governing value of 4.86. To maintain a conservative characteristic-resistance prediction across all investigated brittle-failure configurations, the governing value was rounded upward, and a calibration factor of CF = 4.9 was adopted.

With CF = 4.9, the calibrated RSM predictions remained at or below the estimated 5th-percentile resistances for all investigated brittle-failure configurations. The corresponding prediction ratios ranged from approximately 0.48 to 0.99, with a mean prediction ratio of approximately 0.72. The selected CF should therefore be interpreted as a Balau-specific conservative calibration factor within the experimental domain investigated, rather than as a statistically optimized or universally applicable constant.

The zero-intercept regression between the calibrated RSM predictions and experimental 5th-percentile resistances produced a slope of 0.67 and an uncentered R^2 of 0.96. Because the regression was constrained through the origin, the R^2 value represents the degree of proportional association between predicted and experimental resistances within the calibration dataset and should not be interpreted as evidence of independent predictive validation. Importantly, CF = 4.9 was selected based on the conservative characteristic-resistance envelope rather than by maximizing the regression R^2, ensuring that the RSM predictions did not exceed the estimated 5th-percentile resistances across the investigated brittle-failure configurations.

The same brittle row-shear configurations (Group 5 and Groups 10–18) used to determine CF = 4.9 were subsequently used to assess the agreement of the calibrated RSM with the experimental results in Section 3.2.5. No independent Balau dataset was used for out-of-sample validation in the present study. Consequently, the reported prediction ratio, MAPE, and RMSE for the calibrated RSM represent within-calibration-set agreement and should not be interpreted as independent validation performance. Independent experimental validation using additional Balau specimens and connection configurations is therefore required before CF = 4.9 can be generalized beyond the experimental domain investigated.

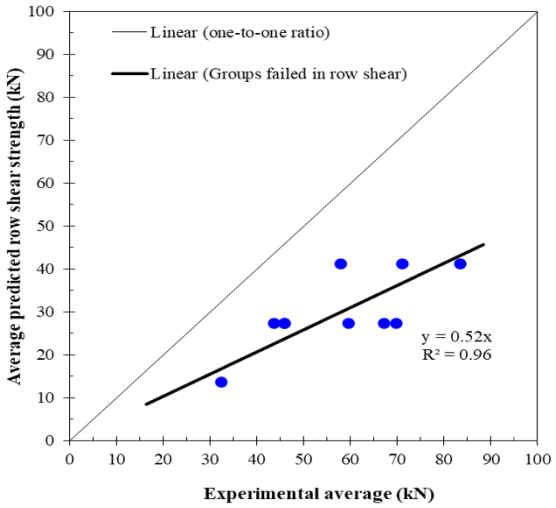

Fig. 11. Calibration of the RSM for Balau wood using a calibration factor of 4.9

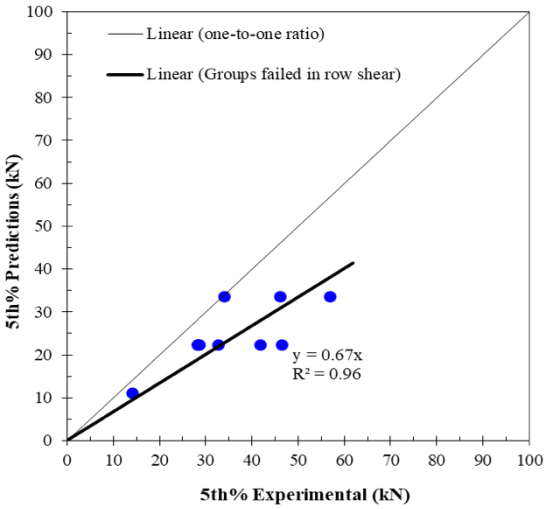

Fig. 12. Zero-intercept regression between RSM predictions and experimental 5th-percentile resistances using CF = 4.9

3.2.5 Predictive Performance under Brittle Failure Mode: RSM versus MS544-5

The predictive performance of the Row Shear Model (RSM) and MS544-5 for connection groups governed by brittle row shear failure (Group 5 and Groups 10–18) is summarized in Table 5 and illustrated in Figure 13. The comparison between predicted strengths and experimentally determined 5th-percentile resistances demonstrates that the RSM consistently provides improved agreement with experimental behavior compared to the current timber code provisions.

The experimentally obtained connection strengths exhibited acceptable statistical consistency, as reflected by the measured coefficients of variation (CoV). The use of 5th-percentile resistance values enables direct comparison with characteristic design-level predictions and ensures consistency with structural reliability principles adopted in timber connection design. The RSM predictions were evaluated using the calibrated factor determined in Section 3.2.4. Shear strength parallel to the grain was estimated from the experimentally measured oven-dry density using the correlation proposed by Abdul Karim et al. [12]. The commonly adopted reduction factor used to convert average values to characteristic strengths was intentionally excluded from the present analysis, since the 5th-percentile density value had already been incorporated directly into the prediction procedure. This avoids excessive conservatism and ensures consistency between experimentally derived material parameters and analytical prediction. For Balau bolted connections, the RSM prediction ratios ranged from 0.48 to 0.99, with a mean prediction ratio of 72%, whereas MS544-5 produced lower prediction ratios ranging from 0.43 to 0.87, corresponding to a mean prediction ratio of 63% (as shown in Table 5). The consistently higher prediction ratios obtained using the RSM indicate that mechanistically based brittle failure formulations provide improved representation of row shear behavior compared with the simplified empirical provisions of MS544-5.

For the brittle row-shear configurations, the calibrated RSM (CF = 4.9) yielded a mean prediction ratio of 0.72, MAPE of 27.88%, and RMSE of 13.57 kN, compared with 0.63, 36.60%, and 16.19 kN, respectively, for MS544-5. The lower MAPE and RMSE indicate smaller deviations of the calibrated RSM from the experimental characteristic resistances within the investigated dataset. These values represent agreement within the calibration dataset and should not be interpreted as independent validation performance. As shown in Figure 13, the RSM predictions exhibit closer alignment with the one-to-one reference line than the MS544-5 predictions, which remain systematically conservative across most connection groups. Both approaches generally maintain conservative prediction trends; however, the calibrated RSM provides closer agreement with the experimental 5th-percentile resistances without producing unconservative overprediction within the investigated configurations. Thus, calibration of the brittle row-shear formulation improved

agreement with the experimental characteristic resistances while maintaining conservative predictions across the investigated dataset.

The closer agreement obtained using the RSM can be attributed to its explicit representation of the governing brittle row-shear mechanism [20,21], in which connection resistance is controlled by timber shear failure parallel to the grain. In contrast, MS544-5 does not explicitly incorporate the mechanics of brittle row-shear failure and therefore has limited sensitivity to the geometric parameters governing this failure mechanism. This mechanistic difference provides a basis for the lower mean prediction ratio obtained using MS544-5 compared with the calibrated RSM.

The experimental results further demonstrate the influence of connection geometry on brittle row-shear behavior. In particular, end distance (e_t) and bolt spacing (s_b) affected the governing failure mechanism, with reduced geometric spacing associated with lower deformation capacity and greater susceptibility to abrupt row-shear failure. These trends are consistent with the experimentally observed failure behavior discussed in Section 3.2.2 and highlight the importance of explicitly considering connection geometry when assessing brittle resistance.

The observed trends are also consistent with previous investigations of Malaysian hardwoods, including Meraka [12,13], Nyatoh [14,15], and Bitis [16], in which brittle shear behavior was influenced by connection geometry and was more explicitly represented by mechanistically based formulations. This consistency across different hardwood species provides further support for the mechanistic basis of the RSM formulation. Nevertheless, the Balau-specific calibration factor established in the present study should be interpreted within the experimental domain investigated and should not be generalized to other species or connection configurations without further experimental assessment. Overall, within the investigated calibration dataset, the calibrated RSM provided closer and more physically consistent agreement with the experimental 5th-percentile resistances than MS544-5. The results demonstrate the value of explicitly incorporating the brittle row-shear mechanism when assessing bolted hardwood connections and support further assessment of mechanistically based row-shear formulations for structural design applications. Independent experimental validation using additional Balau specimens and connection configurations is required before the calibrated factor can be generalized beyond the experimental domain investigated in this study.

Collectively, the predictive trends observed for both ductile and brittle failure modes demonstrate that mechanistically based formulations provide a more representative description of the governing physical behavior of bolted hardwood connections than the simplified empirical code provisions considered in this study. The closer agreement achieved using the EYM and calibrated RSM highlights the importance of explicitly incorporating timber embedding deformation, fastener yielding, and brittle row-shear mechanisms when assessing the resistance and failure behavior of dense tropical hardwood bolted connections.

Table 5. Comparison of RSM and MS544-5 predictions with experimental results for brittle row-shear configurations of Balau bolted connections

Group	Experimental			Predictions		PR		RSM vs MS544-5		
	R_{avg} (kN)	CoV (%)	$R_{5th\%}$ (kN)	RSM (kN)	MS544-5 (kN)	$\frac{RSM}{R_{5th\%}}$	$\frac{MS544\text{-}5}{R_{5th\%}}$	$\overline{PR}$	MAPE (%)	RMSE (kN)
5	32.37	35	14.00	11.24	9.88	0.80	0.71			
10	45.87	23	28.26	22.48	19.76	0.80	0.70			
11	67.10	23	41.71	22.48	19.76	0.54	0.47			
12	69.65	20	46.37	22.48	19.76	0.48	0.43			
13	59.51	27	32.60	22.48	19.76	0.69	0.61	0.72 vs 0.63	27.88 vs 36.60	13.57 vs 16.19
14	45.75	23	28.26	22.48	19.76	0.80	0.70			
15	43.59	21	28.58	22.48	19.76	0.79	0.69			
16	83.34	19	56.90	33.72	29.64	0.59	0.52			
17	70.98	21	45.97	33.72	29.64	0.73	0.64			
18	57.87	25	33.98	33.72	29.64	0.99	0.87			

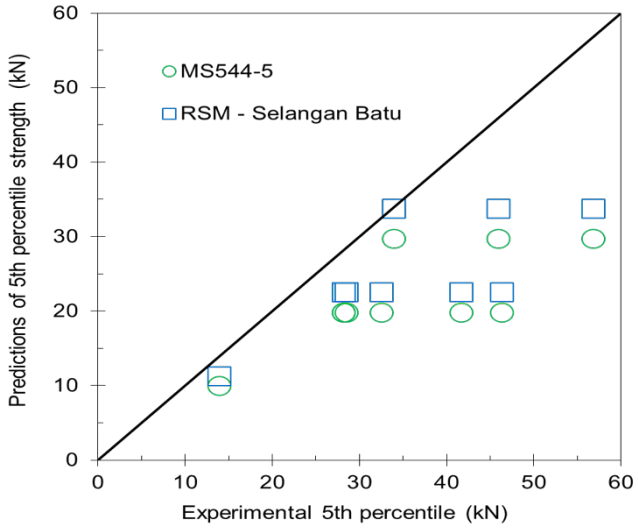

Fig. 13. Comparison of RSM and MS544-5 predictions with experimental 5th-percentile resistances for brittle row-shear configurations

4. Conclusions

This study experimentally investigated the behavior of steel–wood–steel (SWS) bolted connections using Balau wood (Shorea spp.), with emphasis on the prediction of ductile and brittle failure mechanisms relevant to timber diaphragm retrofit applications in unreinforced masonry (URM) structures [5,10]. The experiments were conducted under monotonic loading; therefore, the findings characterize the monotonic strength, deformation behavior, and failure mechanisms of the investigated connections and should not be interpreted as direct evidence of their cyclic or seismic performance.

The results demonstrated that connection behavior was governed by a transition between embedding-controlled ductile response and brittle row-shear failure, primarily influenced by geometric parameters such as end distance and bolt spacing. Connections with reduced geometric spacing exhibited greater susceptibility to brittle failure and lower deformation capacity. The ductile behavior observed under monotonic loading is relevant to timber diaphragm retrofit applications where connection deformation capacity is an important design consideration. However, monotonic ductility alone does not establish seismic energy-dissipation capacity or hysteretic performance. For ductile failure modes, the European Yield Model (EYM) provided closer agreement with the experimental characteristic strengths than MS544-5, demonstrating the importance of incorporating embedding-strength-based mechanics when assessing dense tropical hardwood connections. For brittle failure modes, the calibrated Row Shear Model (RSM) provided closer agreement with the experimental characteristic strengths than MS544-5, highlighting the importance of explicitly accounting for row-shear mechanisms and species-specific calibration in timber connection modelling. The prediction ratio, MAPE, and RMSE further quantified the relative agreement of these analytical approaches with the experimental results. For the calibrated RSM, these measures represent agreement within the calibration dataset rather than independent out-of-sample validation.

Overall, the findings demonstrate that mechanistically based analytical models can provide a more representative assessment of the observed ductile and brittle resistance mechanisms than the simplified empirical provisions considered in this study. The proposed framework contributes towards the more reliable assessment and design of bolted connections using tropical hardwoods and provides a useful basis for their consideration in timber diaphragm retrofit systems for URM structures. Nevertheless, because the present investigation was limited to monotonic loading, dedicated reversed-cyclic testing is required before conclusions can be drawn regarding seismic performance. Future studies should therefore evaluate hysteretic response, strength and stiffness degradation, cumulative damage, and energy-dissipation capacity under cyclic loading representative of seismic demands.

Acknowledgement

The authors acknowledge the funding support from the Ministry of Higher Education Malaysia under fundamental research grant scheme FRGS/1/2022/TK06/UNIMAS/02/2, and Universiti Malaysia Sarawak (UNIMAS) for the support provided towards this publication. Appreciation is also extended to the Forest Department Sarawak for Balau wood identification and to the Faculty of Engineering, UNIMAS, for access to testing facilities.

References

[1] Griffith MC. Performance of unreinforced masonry buildings during the Newcastle earthquake, Australia. Adelaide (Australia): The University of Adelaide; 1991. Research Report No. R86.
[2] Blaikie EL, Spurr DD. Earthquake vulnerability of existing unreinforced masonry buildings. Wellington (New Zealand): Works Consultancy Services; 1992.
[3] Bruneau M. State-of-the-art report on seismic performance of unreinforced masonry buildings. J Struct Eng. 1994;120(1):230-51. https://doi.org/10.1061/(ASCE)0733-9445(1994)120:1(230
[4] Bothara JK, Dhakal RP, Mander JB. Seismic performance of an unreinforced masonry building: an experimental investigation. Earthq Eng Struct Dyn. 2009;39(1):45-68. https://doi.org/10.1002/eqe.932
[5] Abdul Karim AR, Quenneville P, Sa'don NM. Design optimization of the bolted connection loaded parallel to the timber grain for masonry building retrofits. Int J Mech. 2022;16:6-14. https://doi.org/10.46300/9104.2022.16.2
[6] Fauzan, Hakam A, Ismail FA, Osman JV, Jauhari ZA. Experimental investigation of hollow brick unreinforced masonry building retrofitted by ferrocement layers. Int J Geomate. 2023;24(102). https://doi.org/10.21660/2023.102.s8622
[7] Ismail N, Khattak N. Observed failure modes of unreinforced masonry buildings during the 2015 Hindu Kush earthquake. Earthq Eng Eng Vib. 2019;18(2):301-14. https://doi.org/10.1007/s11803-019-0505-x
[8] Dizhur D, Ingham J, Moon L, Griffith M, Schultz A, Senaldi I, et al. Performance of masonry buildings and churches in the 22 February 2011 Christchurch earthquake. Bull N Z Soc Earthq Eng. 2011;44(4):279-96. https://doi.org/10.5459/bnzsee.44.4.279-296
[9] Dizhur D, Ismail N, Knox C, Lumantarna R, Ingham JM. Performance of unreinforced and retrofitted masonry buildings during the 2010 Darfield earthquake. Bull N Z Soc Earthq Eng. 2010;43(4):321-39. https://doi.org/10.5459/bnzsee.43.4.321-339
[10] Abdul Karim AR. Seismic assessment of wall-diaphragm connections in New Zealand unreinforced masonry buildings [dissertation]. Auckland (New Zealand): The University of Auckland; 2012.
[11] Department of Standards Malaysia. Code of practice for structural use of timber: part 5: timber joints (first revision). Cyberjaya (Malaysia): Department of Standards Malaysia; 2018. Report No.: MS544-5.
[12] Abdul Karim AR, Quenneville P, M.Sa'don N, Yusof M. Investigating the Meraka hardwood failure in bolted connections parallel to the timber grain. Int J Eng Technol. 2018;7(3.18):62-5. https://doi.org/10.14419/ijet.v7i3.18.16675
[13] Abdul Karim AR, Quenneville P, Sa'don NM. Shear failure of the Meraka hardwood in bolted connections loaded parallel to the timber grain. IOP Conf Ser Mater Sci Eng. 2021;1101(1):012005. https://doi.org/10.1088/1757-899X/1101/1/012005
[14] Ujan XL, Karim ARA, Sa'don NM, Teng XY, Quenneville P, Rahim NL. Effectiveness validation on existing design equations for the sustainable design of masonry building retrofits. J Sustain Sci Manag. 2022;17(6):79-91. https://doi.org/10.46754/jssm.2022.06.007
[15] Ujan XL, Karim ARA, Sa'don NM, Sahari SH, Rahim NL, Quenneville P. Validation of shear failure on bolted connection for Nyatoh hardwood. J Eng Sci Technol. 2023;18(5):2398-410.
[16] Sukarman E, Abdul Karim AR, M.Sa'don N, Abdullah AA, Sahari SH, Rahim NL, et al. Evaluating the SWS bolted connection strength of Bitis wood. Res Eng Struct Mater. 2023;10.
[17] Quenneville P. Design of bolted connections: a comparison of a proposal and various existing standards. J Struct Eng Soc N Z Inc. 2009;22(2):57-62.
[18] Sawata K. Strength of bolted timber joints subjected to lateral force. J Wood Sci. 2015;61(3):221-9. https://doi.org/10.1007/s10086-015-1469-8
[19] Quenneville JHP, Jensen J. Validation of the Canadian bolted connection design proposal. In: Proceedings of the CIB-W18 Meeting; 2008.
[20] Jockwer R, Fink G, Köhler J. Assessment of the failure behaviour and reliability of timber connections with multiple dowel-type fasteners. Eng Struct. 2018;172:76-84. https://doi.org/10.1016/j.engstruct.2018.05.081
[21] Yurrita M, Cabrero JM. New design model for brittle failure in the parallel-to-grain direction of timber connections with large diameter fasteners. Eng Struct. 2020;217:110557. https://doi.org/10.1016/j.engstruct.2020.110557

[22] Lokaj A, Dobes P, Sucharda O. Effects of loaded end distance and moisture content on the behavior of bolted connections in squared and round timber subjected to tension parallel to the grain. Materials. 2020;13(23):5525. https://doi.org/10.3390/ma13235525
[23] Cao J, Xiong H, Liu Y. Experimental study and analytical model of bolted connections under monotonic loading. Constr Build Mater. 2021;270:121380. https://doi.org/10.1016/j.conbuildmat.2020.121380
[24] Forest Products Laboratory. Wood handbook: wood as an engineering material. Madison (WI): U.S. Department of Agriculture, Forest Service; 2021.
[25] Department of Standards Malaysia. Code of practice for structural use of timber: part 2: permissible stress design of solid timber (first revision). Cyberjaya (Malaysia): Department of Standards Malaysia; 2017. Report No.: MS544-2.
[26] Malaysian Timber Industry Board. Specifying timber for building construction: strength groups of timber and their applications [Internet]. Kuala Lumpur: Malaysian Timber Industry Board, Ministry of Plantation and Commodities; [cited 2025 Jun 28]. Available from: https://www.mtib.gov.my/en/procurement?view=article&id=64%3Aspecifying-timber-for-building-construction&catid=2
[27] Chu Fei FT. Anatomical features of the Dipterocarp timber of Sarawak. Gard Bull Singapore. 1974;27:1-20.
[28] The Wood Database. Balau - lumber identification (hardwood) [Internet]. The Wood Database; [cited 2025 May 7]. Available from: https://www.wood-database.com/balau/
[29] Standards New Zealand. Timber - methods of test - method 1: moisture content. Wellington (New Zealand): Standards New Zealand; 2012. Standard No.: AS/NZS 1080.1.
[30] Standards New Zealand. Timber - methods of test - method 3: density. Wellington (New Zealand): Standards New Zealand; 2000. Standard No.: AS/NZS 1080.3.
[31] International Organization for Standardization. Timber structures - dowel-type fasteners - part 2: determination of embedding strength and foundation values. Geneva (Switzerland): International Organization for Standardization; 2009. Standard No.: ISO/DIS 10984-2.
[32] International Organization for Standardization. Timber structures - joints made with mechanical fasteners - general principles for the determination of strength and deformation characteristics. Geneva (Switzerland): International Organization for Standardization; 1983. Standard No.: ISO 6891.